Available online at www.sciencedirect.com
SCIENCE DIRECT®
Planetary and Space Science 51 (2003) 1017–1033
Planetary and Space Science
www.elsevier.com/locate/pss

Chemical sources of haze formation in Titan's atmosphere

E.H. Wilson[a,*], S.K. Atreya[b]

[a] NASA/Jet Propulsion Laboratory, 4800 Oak Grove Drive M/S 169-237, Pasadena, CA 91109-8099, USA
[b] Department of Atmospheric, Oceanic, and Space Sciences, University of Michigan, Ann Arbor, 2455 Hayward Street, Ann Arbor, MI 48109-2143, USA

Received 16 January 2003; received in revised form 20 June 2003; accepted 23 June 2003

Abstract

A prominent feature of Titan's atmosphere is a thick haze region that acts as the end product of hydrocarbon and nitrile chemistry. Using a one-dimensional photochemical model, an investigation into the chemical mechanisms responsible for the formation of this haze region is conducted. The model derives profiles for Titan's atmospheric constituents that are consistent with observations. Included is an updated benzene profile that matches more closely with—recent ISO observations (Icarus 161 (2003) 383), replacing the profile given in the benzene study of Wilson et al. (J. Geophys. Res. 108 (2003) 5014). Using these profiles, pathways from polyynes, aromatics, and nitriles are considered, as well as possible copolymerization among the pathways. The model demonstrates that the growth of polycyclic aromatic hydrocarbons throughout the lower stratosphere plays an important role in furnishing the main haze layer, with nitriles playing a secondary role. The peak chemical production of haze layer ranges from 140 to 300 km peaking at an altitude of 220 km, with a production rate of 3.2×10^{-14} g cm^{-2} s^{-1}. Possible mechanisms for polymerization and copolymerization and suggestions for further kinetic study are discussed, along with the implications for the distribution of haze in Titan's atmosphere.

Keywords: Titan; Atmospheric composition; Photochemistry; Organic chemistry

1. Introduction

The surface of Titan is shrouded by a thick haze region (Smith et al., 1981; Rages et al., 1983), a prominent feature in Titan's opaque atmosphere. This region is split into a main haze layer that resides below ~ 220 km and a detached layer at 300–350 km (Rages and Pollack, 1983). Microphysical models place the altitude of peak aerosol production anywhere from 250 to 600 km (Rannou et al., 1997, and all references within), while Chassefière and Cabane (1995) suggest two formation regions for the main haze layer (350–400 km) and detached haze layer (500–800 km), through different chemical mechanisms. These models, using high-phase-angle images (Rages et al., 1983) and Infrared Spectrometer (IRIS) data from Voyager and geometric albedos (Neff et al., 1985; Fink and Larson, 1979), have derived the haze production rate in the range of $0.5–2 \times 10^{-14}$ g cm^{-2} s^{-1} (McKay et al., 2001).

However, the precise sources and mechanisms for the formation of hazes in Titan's atmosphere are quite uncertain. Laboratory simulations of Titan's atmospheric conditions have sought to answer this question through the analysis of tholins (Sagan and Khare, 1979), brown complex solid organics produced through the irradiation of organic molecules by UV light or electrical discharge. These simulations have provided some insight into the nature of molecules and the mechanisms that accompany the formation of sub-micron particles. For instance, laboratory simulations have shown that formation of aerosol particles result from photolysis of acetylene (C_2H_2), ethylene (C_2H_4), and hydrogen cyanide (HCN) (Scattergood, 1995; Bar-Nun et al., 1988). However, limitations in experimental conditions restrict the ability of laboratory simulations to fully represent the energy sources and transport that affect Titan's atmospheric constituents.

Photochemical models have attempted to take these considerations into account in analyzing the pathways that form haze particles. Unfortunately, laboratory measurements of the kinetics of reactions directly leading to the formation of haze particles under Titanian atmospheric conditions are not available. Nevertheless, an examination of the

* Corresponding author. Tel.: +1-818-354-9971; fax: +1-818-393-4619.
E-mail address: eric.wilson@jpl.nasa.gov (E.H. Wilson).

0032-0633/$ - see front matter © 2003 Elsevier Ltd. All rights reserved.
doi:10.1016/j.pss.2003.06.003

precursory processes to haze formation can provide clues into the composition and formation region of Titan haze. Nitrogen (N_2) and methane (CH_4) predominate Titan's composition and, through dissociation, provide the foundation of Titan's organic-producing laboratory. The possible formation of haze particles through polyyne formation (Yung et al., 1984; Toublanc et al., 1995; Lara et al., 1996) and through polymerization of the nitrile HCN (Banaszkiewicz et al., 2000) in Titan photochemistry has been examined. However, previous Titan photochemical models have given little attention to the aromatic pathway, anchored by the formation of benzene (C_6H_6), which has been tentatively identified in Titan's atmosphere (Coustenis et al., 2003). Wilson and Atreya (2001) and Wilson (2002), examining polyyne, aromatic, and nitrile mechanisms, suggested that this aromatic pathway may be the primary route to Titan haze formation. Lebonnois et al. (2002) have also studied possible chemical routes to Titan haze through nitrile and aromatic polymers as well as cyanoacetylene/acetylene copolymers. In the following sections, we update this investigation into the formation of haze via the polyyne, aromatic, and nitrile pathways as well as examine possible mechanisms for copolymerization among these pathways in order to gain insight into the mechanisms that are responsible for the presence of the Titan haze region and its composition. A list of important reaction rates used in this study is provided in Table 1.

2. Pure polyacetylene polymers

The polymerization of acetylene (C_2H_2) through polyyne formation has been postulated as a possible vehicle for the creation of haze particles in the atmosphere of Titan (Allen et al., 1980). This polyyne process is initiated with the photodissociation of acetylene, creating ethynyl radical (C_2H) through hydrogen abstraction. C_2H proceeds to react with another acetylene molecule to produce diacetylene (C_4H_2)

$$C_2H_2 + C_2H \rightarrow C_4H_2 + H, \qquad (R1)$$

and the process continues, forming ever-larger successive polyacetylenes C_6H_2, C_8H_2, etc.

$$C_{2n}H_2 + C_2H \rightarrow C_{2n+2}H_2 + H, \quad n = 1, 2, 3, \ldots . \qquad (R2)$$

Such polyynes have been identified as major hydrocarbon intermediates in pyrolysis processes at high temperatures and soot production (Kiefer and von Drasek, 1990; Krestinin, 2000). These long chain polyynes also photodissociate and produce polyacetylene radicals (e.g. C_4H, C_6H), which play the same role as C_2H in creating longer chains. Under pyrolytic conditions, H-elimination causes the formation of radical sites, upon which further polyyne building can continue. This "breeding" process can result in cyclization of the complex, shown in Fig. 1, rather than a lengthening of the chain, eventually causing nucleation of the soot particle (Krestinin, 2000).

The low activation energy of the ethynyl-insertion into acetylene followed by H-abstraction mechanism allows (R1) to proceed efficiently at low temperatures, as well (Chastaing et al., 1998). However, kinetic data of polyyne formation above the C_4 variety are not available, necessitating assumptions for rate coefficients. Yung et al. (1984) assumed that these polyacetylenes were precursors of soot and followed the fate of polyacetylenes in Titan's atmosphere up to C_8H_2. Acknowledging that (R2) will likely proceed in a manner similar to (R1), Yung et al. assumed that larger polyacetylene radicals will be less reactive than C_2H, using a formulation

$$k(C_{2n}H) = 3^{1-n}k(C_2H), \quad n = 1, 2, 3.$$

At higher temperatures, these radicals are assumed to proceed at similar rates to C_2H (Frank and Just, 1980; Kiefer and von Drasek, 1990). $C_{2n}H_2$-elimination to produce $C_{2n+2}H_2$ is not the primary loss process for these molecules. Thus, to determine the upper limit of polyacetylene-polymer (PA-polymer) production, the following assumption is adopted

$$k(C_{2n}H + X) = k(C_2H + X), \quad n = 2, 3, \ldots,$$

$$X = H_2, CH_4, C_2H_2, \ldots .$$

The basis for the lengthening of polyacetylenic chains is set by (R1). This reaction has been recently measured by Chastaing et al. (1998), using a CRESU (Cinétique de Réaction en Ecoulement Supersonique Uniforme) apparatus, which measures rate coefficients down to 15 K. Fitting their data points measured from 295 to 39 K, we obtained a rate expression of $9.53 \times 10^{-11}\ e^{30.8/T}\ cm^3\ s^{-1}$. This expression gives rate coefficients for (R1) twice as high as those used in the Toublanc et al. (1995) and Lara et al. (1996) models and 4 times as high as that used in Yung et al. (1984) model in the temperature region where chemistry plays an important role on Titan. This chain-lengthening process is continued through the photolysis of C_4H_2

$$C_4H_2 + h\nu \rightarrow C_4H + H \qquad (J1a)$$

$$\rightarrow C_2H + C_2H \qquad (J1b)$$

$$\rightarrow C_2H_2 + C_2 \qquad (J1c)$$

$$\rightarrow C_4H_2. \qquad (J1d)$$

Glicker and Okabe (1987) measured C_4H_2 photolytic quantum yields to be

$$\lambda < 1650\ \text{Å} : q_{J1a} = 0.2, q_{J1b} = 0.03,$$

$$q_{J1c} = 0.1, q_{J1d} = 0.67, 1650\ \text{Å} \leqslant \lambda < 2050\text{Å} : q_{J1b} = 0.01,$$

$$q_{J1c} = 0.06, q_{J1d} = 0.93, \quad \lambda \geqslant 2050\ \text{Å} : q_{J1d} = 1.0.$$

Table 1
Rate coefficients for important reactions in this study

Reactions	Rate coefficients[a,b]	References
Polyyne chemistry		
$C_2H + C_2H_2 \rightarrow C_4H_2 + H$	$9.5 \times 10^{-11}\ e^{30.8/T}$	Chastaing et al. (1998)
$C_2H + C_8H_2 \rightarrow$ PA-polymer	$9.5 \times 10^{-11}\ e^{30.8/T}$	Estimated, $k(C_2H + C_2H_2)$; see text
$C_4H + C_6H_2 \rightarrow$ PA-polymer	$9.5 \times 10^{-11}\ e^{30.8/T}$	Estimated, $k(C_2H + C_2H_2)$; see text
$C_4H + C_8H_2 \rightarrow$ PA-polymer	$9.5 \times 10^{-11}\ e^{30.8/T}$	Estimated, $k(C_2H + C_2H_2)$; see text
$C_6H + C_4H_2 \rightarrow$ PA-polymer	$9.5 \times 10^{-11}\ e^{30.8/T}$	Estimated, $k(C_2H + C_2H_2)$; see text
$C_6H + C_6H_2 \rightarrow$ PA-polymer	$9.5 \times 10^{-11}\ e^{30.8/T}$	Estimated, $k(C_2H + C_2H_2)$; see text
$C_6H + C_8H_2 \rightarrow$ PA-polymer	$9.5 \times 10^{-11}\ e^{30.8/T}$	Estimated, $k(C_2H + C_2H_2)$; see text
Aromatic chemistry		
$C_3H_3 + C_3H_3 + M \rightarrow n\text{-}C_6H_6 + M$	$k_0 = 8.76 \times 10^{-6} T^{-7.03}\ e^{-1390/T}$ $k_\infty = 4.0 \times 10^{-11}$	k_0 estimated; Wang and Frenklach (1997)
(a) $n\text{-}C_6H_6 + H \rightarrow C_6H_6 + H$ (b) $+M \rightarrow n\text{-}C_6H_7 + M$	$k_a = 1.44 \times 10^{-7} T^{-1.34}\ e^{-1762/T}$ $k_{b0} = 8.0 \times 10^{-31} T^{-0.52}\ e^{-504/T}$ $k_{b\infty} = 1.06 \times 10^{-14} T^{0.86}\ e^{-554/T}$	Wang and Frenklach (1994)
(a) $C_4H_3 + C_2H_2 + M \rightarrow C_6H_5 + M$ (b) $\rightarrow n\text{-}C_6H_5 + M$	$k_{a0} = 1.3 \times 10^{10} T^{-12.77}\ e^{-5888/T}$ $k_{a\infty} = 2.8 \times 10^{-17} T^{0.47}\ e^{-3020/T}$ $k_{b0} = 2.2 \times 10^{-24} T^{-2.66}\ e^{-1711/T}$ $k_{b\infty} = 4.8 \times 10^{-17} T^{1.40}\ e^{-1158/T}$	Wang and Frenklach (1994)
$C_4H_5 + C_2H_2 \rightarrow C_6H_6 + H$	$k = 3.16 \times 10^{-17} T^{1.47}\ e^{-2471/T}$	Westmoreland et al. (1989)
$C_6H_5 + H + M \rightarrow C_6H_6 + M$	$k_0 = 1.82 \times 10^{28} T^{-16.3}\ e^{-3526/T}$ $k_\infty = 1.66 \times 10^{-10}$	Wang and Frenklach (1997)
(a) $C_6H_6 + H \rightarrow C_6H_5 + H_2$ (b) $+M \rightarrow C_6H_7 + M$	$k_a = 4.15 \times 10^{-10}\ e^{-8052/T}$ $k_{b0} = 1.0 \times 10^{-28}$ $k_{b\infty} = 5.27 \times 10^{-11}\ e^{-1605/T}$	Wang and Frenklach (1997); k_{b0} estimate; Mebel et al. (1997)
(a) $C_6H_5 + C_2H_2 \rightarrow$ PAH-polymer (b) $+M \rightarrow$ PAH-polymer	$k_a = 3.72 \times 10^{-13}\ e^{-1560/T}$ $k_{b0} = 4.97 \times 10^{-19} T^{-4.08}\ e^{-403/T}$ $k_{b\infty} = 6.64 \times 10^{15} T^{-8.94}\ e^{-6039/T}$	Yu et al. (1994); Wang and Frenklach (1994)
$C_6H_6 + C_6H_5 \rightarrow$PAH-polymer	$k = 1.59 \times 10^{-12}\ e^{-2168/T}$	Park et al. (1999)
Nitrile chemistry		
$HCN + C_2H_3 \rightarrow C_2H_3CN + H$	$1.1 \times 10^{-12}\ e^{-900/T}$	Monks et al. (1993); see text
$CN + C_2N_2 \rightarrow$ NT-polymer	$2.19 \times 10^{-21} T^{2.7}\ e^{-770/T}$	Yang et al. (1992)
$CN + C_2H_3CN \rightarrow$ NT-polymer	4.23×10^{-11}	Butterfield et al. (1993)
$CN + C_4N_2 \rightarrow$ NT-polymer	5.4×10^{-13}	Seki et al. (1996)
$H_2CN + HCN \rightarrow$ NT-polymer	$10^{-3} \times 1.1 \times 10^{-12}\ e^{-900/T}$	Estimated, $k(HCN + C_2H_3)$; see text
Copolymer reactions		
$HC_3N + C_2H \rightarrow$ products	$3.32 \times 10^{-12}\ e^{-2516/T}$	Estimated, $k(C_2H_2 + C_2H)$ from Chastaing et al. (1998)
$HC_3N + C_2H_3 \rightarrow$ products	$4.17 \times 10^{-19} T^{1.9}\ e^{-1058/T}$	Estimated, $k(C_2H_2 + C_2H_3)$ from Weissmann and Benson (1988)
$HC_3N + C_2H_5 \rightarrow$ products	$8.32 \times 10^{-14}\ e^{-3520/T}$	Estimated, $k(C_2H_2 + C_2H_5)$ from Kerr and Parsonage (1972)
$HC_3N + C_6H_5 \rightarrow$ Co-polymer	$3.72 \times 10^{-13}\ e^{-1560/T}$	Estimated, $k(C_6H_5 + C_2H_2)$
$HC_3N^* + C_2H_2 \rightarrow$ Co-polymer	$1.28 \times 10^{-12} T^{0.5}$	Estimated, $k(C_4H_2^* + C_2H_2)$ from Frost et al. (1996)

[a]All rate coefficients are in units of $cm^3\ s^{-1}$, except those denoted by k_0, which are in units of $cm^6\ s^{-1}$.
[b]Three-body reactions are calculated according to the expression $k = k_0 k_\infty M/(k_0 M + k_\infty)$.

Along with polyacetylenic radicals, metastable diacetylene also contributes in forming higher-order polyynes. This process occurs through the reaction of metastable diacetylene, $C_4H_2^*$, with acetylene and diacetylene (Frost et al., 1995; Bandy et al., 1993). Such reactions comprise 40% of the total C_6H_2 formation and 22% of the total C_8H_2 formation.

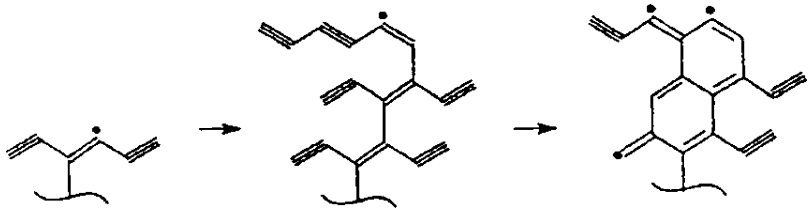

Fig. 1. Formation of a polyyne complex on a surface radical site, and its transformation into a more stable structure, followed by "breeding" of radical sites. (after Krestinin, 2000).

The main obstacle to any possible acetylene polymerization is acetylenic recycling, which proceeds through the reaction of C_2H with CH_4, C_2H_4, C_2H_6, and C_3H_8

$$C_2H + H_2 \rightarrow C_2H_2 + H, \quad \text{(R3)}$$

$$C_2H + CH_4 \rightarrow C_2H_2 + CH_3, \quad \text{(R4)}$$

$$C_2H + H_2H_4 \rightarrow C_2H_2 + C_2H_3, \quad \text{(R5)}$$

$$C_2H + C_2H_6 \rightarrow C_2H_2 + C_2H_5, \quad \text{(R6)}$$

$$C_2H + C_3H_8 \rightarrow C_2H_2 + C_3H_7. \quad \text{(R7)}$$

Of these reactions, (R4) and (R6) are the most important in Titan's atmosphere. Opansky and Leone (1996a, b) conducted low temperature measurements of rate coefficients for (R4) and (R6), obtaining a rate coefficient an order of magnitude larger than that used by Lara et al. (1996). This would result in a more efficient recycling mechanism, although there is agreement among all Titan models that (R4) is the most important recycler.

C_6H_2 has not yet been identified in the atmosphere of Titan, but laboratory simulations at Titan-like conditions (100–150 K) (de Vanssay et al., 1995) have detected C_6H_2 at an abundance of 2–7 $\times$ 10^{-2} relative to C_4H_2. In the region where this temperature range applies and polyyne distribution is governed by chemistry (400–700 km), we find good agreement, with a C_6H_2 column abundance of 2.3 $\times$ 10^{-2} relative to C_4H_2 in this region, evidence that polyyne chain-lengthening does indeed occur at low temperatures.

Fig. 2 shows the degree at which the density of successive polyacetylenes falls off, rendering any possible stratospheric haze formed from this mechanism minimal. The peak mole fraction of these compounds occur near the 10^{-5} mbar region, making the polyacetylene pathway a possible candidate for the precursors of the detached haze layer, located at higher altitudes, although the low mole fractions of C_6H_2 and C_8H_2, even at high altitudes, argue against this scenario. Assuming all of the production of polyynes containing 10 C atoms and more to result in the formation of PA-polymer,

$$C_6H_2 + C_4H \rightarrow \text{PA-polymer}, \quad \text{(R8)}$$

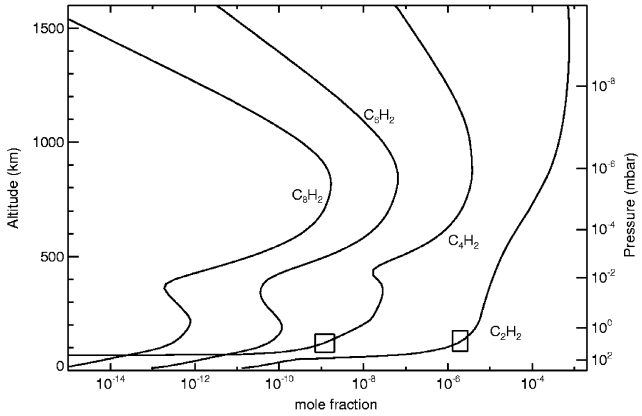

Fig. 2. Abundance profiles for C_4H_2, C_6H_2, and C_8H_2. The rectangles represent the IRIS observations (Coustenis et al., 1989).

$$C_6H_2 + C_6H \rightarrow \text{PA-polymer}, \quad \text{(R9)}$$

$$C_8H_2 + C_2H \rightarrow \text{PA-polymer}, \quad \text{(R10)}$$

$$C_8H_2 + C_4H \rightarrow \text{PA-polymer}, \quad \text{(R11)}$$

$$C_8H_2 + C_6H \rightarrow \text{PA-polymer}, \quad \text{(R12)}$$

and eventually to Titan haze, the resulting haze precursor column output from this pathway is 8.7 $\times$ 10^2 cm^{-2} s^{-1}, peaking at the millibar region in the lower stratosphere, with a larger peak at 10^{-4} mbar. (R10) is responsible for 39% of PA-polymer formation, with (R8) accounting for 29%.

3. Pure nitrile polymers

3.1. Nitrile abundances

The existence of N_2 and CH_4 as the main constituents of Titan's atmosphere suggests the status of nitriles as important contributors to the formation of haze particles. The most abundant nitrile, HCN, is formed in the upper atmosphere as a result of N_2 and CH_4 photolysis

$$0.5(N_2 + h\nu \rightarrow N^{4s} + N^{4s}),$$

$$CH_4 + h\nu \rightarrow CH_3 + H,$$

$$N^{4s} + CH_3 \rightarrow H_2CN + H,$$

$$\underline{H_2CN + H \rightarrow HCN + H_2}$$

$$0.5N_2 + CH_4 \rightarrow HCN + H_2 + H. \quad \text{(S1)}$$

HCN polymers have been proposed to exist readily in the solar system, accounting for phenomena such as the dark surface of comet Halley and the orange–brown clouds of Jupiter and Saturn (Matthews, 1995). Polymerization can be initiated through the reaction of HCN with an excited HCN molecule, producing an HCN dimer, $(HCN)_2$, (Rettig et al., 1992) eventually resulting in poly-HCN, $(HCN)_n$. However, this process is not well understood, and laboratory studies from Khare et al. (1994) suggest that the optical constants of Titan haze do not match those of pure HCN polymers. Lara et al. (1999) analyzed the incorporation of N atoms into Titan haze through the possible polymerization of HCN. Arguing that the neglect of consideration of HCN loss to haze is responsible for their model's overprediction of HCN abundance from 100 to 300 km, Lara et al. found a production rate for haze from HCN sufficient to reduce the HCN density to match observations. Lebonnois et al. (2001) include 2D dynamics as a supplement to vertical eddy diffusion to account for constituent transport and derive a HCN mole fraction profile at the equator that is consistent with observations, arguing that seasonal variations significantly impact HCN distribution. The attempt to derive a one-dimensional eddy diffusion profile (Wilson and Atreya, 2002) that results in constituent profiles consistent with observations yields the profile shown in Fig. 3a. The corresponding HCN profile (Fig. 3b) shows that we do not find the incorporation of N to the haze necessary to fit observations.

Nevertheless, photolysis of HCN does result in the formation of long-chain nitriles, analogous to polyacetylenes, through the action of CN. CN acts in a similar fashion as C_2H, reacting with hydrocarbons and other nitriles to form larger nitrile molecules, such as cyanoacetylene (HC_3N), acrylonitrile (C_2H_3CN), and dicyanoacetylene (C_4N_2). Thompson and Sagan (1989) postulated the formation of heteropolymers through the attachment of —CN and —RCN chains onto nitrile compounds, as shown in Fig. 4. The gas-phase buildup of some of those nitrile compounds through CN addition has been kinetically studied. HC_3N is produced primarily through the addition of the photolytic product CN and acetylene in the upper atmosphere

$$\begin{aligned} &HCN + h\nu \rightarrow CN + H, \\ &\underline{CN + C_2H_2 \rightarrow HC_3N + H} \quad . \\ &HCN + C_2H_2 \rightarrow HC_3N + H \end{aligned} \quad \text{(S2)}$$

The path to ever-larger nitrile molecules can continue in the same manner to form C_4N_2

$$CN + HC_3N \rightarrow C_4N_2 + H. \quad \text{(R13)}$$

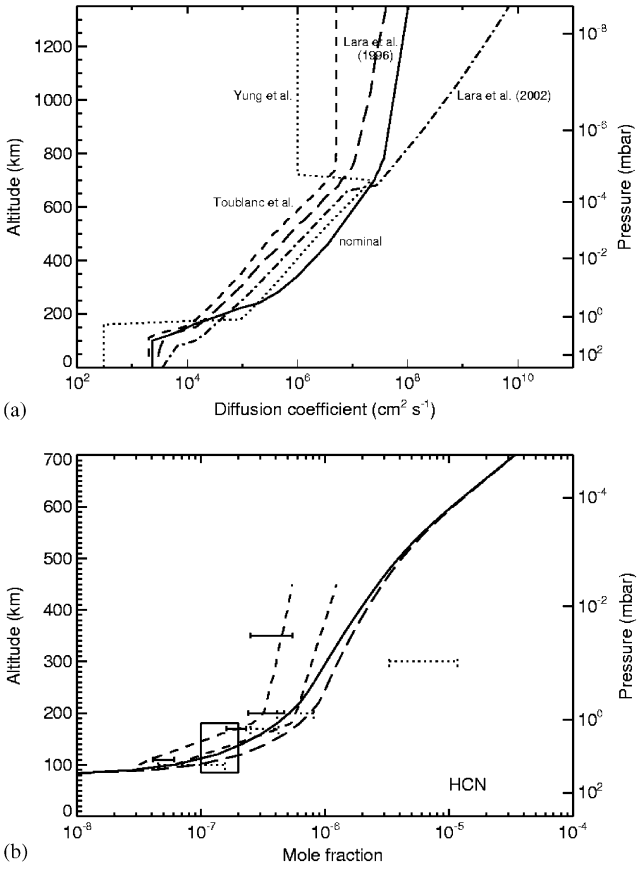

Fig. 3. (a) Eddy diffusion coefficients from the nominal model (solid line), Yung et al. (1984) (dotted line), Toublanc et al. (1995) (short-dashed line), Lara et al. (1996) (long-dashed line), and Lara et al. (2002) (dot–dashed line). (b) HCN profiles with (solid line) and without (long-dashed line) nitrile pathway to haze. Solid bars represent the Hidayat et al. (1997) HCN observations, while the dotted bars represent the Tanguy et al. (1990) observations, and the short-dashed lines represent the profile retrieved from the Marten et al. (2002) observations.

Yung (1987) proposed another mechanism for the formation of C_4N_2 as well as C_2N_2 through the action of the CHCN radical in the reactions

$$CHCN + CHCN \rightarrow C_4N_2 + H_2, \quad \text{(R14)}$$

$$CHCN + N^{4s} \rightarrow C_2N_2 + H. \quad \text{(R15)}$$

Considering estimations by Yung for (R15), the main source of dicyanoacetylene is the scheme

$$\begin{aligned} &N_2 + h\nu \rightarrow 2N^{2d}, \\ &2[N^{2d} + C_2H_2 \rightarrow CHCN + H], \\ &\underline{CHCN + CHCN \rightarrow C_4N_2 + H_2}, \\ &N_2 + 2C_2H_2 \rightarrow C_4N_2 + 2H + H_2 \end{aligned} \quad \text{(S3)}$$

responsible for 98% of C_4N_2 production throughout Titan's atmosphere. Likewise, C_2N_2 is produced through the

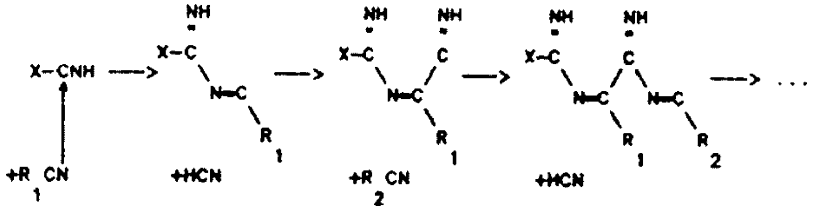

Fig. 4. Nitrile polymerization process involving the formation of chains by the attachment of —CN and —RCN fragments (after Thompson and Sagan, 1989).

scheme

$$\begin{aligned} &N_2 + h\nu \rightarrow N^{4s} + N^{2d},\\ &N^{2d} + C_2H_2 \rightarrow CHCN + H,\\ &\underline{N^{4s} + CHCN \rightarrow C_2N_2 + H_2}\\ &N_2 + C_2H_2 \rightarrow C_2N_2 + 2H \end{aligned} \qquad \text{(S4)}$$

responsible for virtually all of C_2N_2 production. Above 400 km, C_2H_3CN production follows along the same lines as (S2),

$$\begin{aligned} &HCN + h\nu \rightarrow CN + H,\\ &\underline{CN + C_2H_4 \rightarrow C_2H_3CN + H},\\ &HCN + C_2H_4 \rightarrow C_2H_3CN + 2H \end{aligned} \qquad \text{(S5)}$$

while in the lower atmosphere, C_2H_3CN is produced through

$$\begin{aligned} &C_2H_2 + H \xrightarrow{M} C_2H_3,\\ &\underline{HCN + C_2H_3 \rightarrow C_2H_3CN + H}\\ &HCN + C_2H_2 \rightarrow C_2H_3CN + H \end{aligned} \qquad \text{(S6)}$$

Abundance profiles for these nitriles can be found in Fig. 5a.

The most abundant of these nitriles in the lower stratosphere, according to model results in C_2H_3CN. However, C_2H_3CN has not been identified in Titan's atmosphere by IRIS or the Infrared Space Observatory (ISO). In addition, recent millimeter observations from the IRAM telescope derive an upper limit abundance of 2.0×10^{-9} for acrylonitrile (Hidayat, 1997; Marten et al., 2002). Furthermore, Coll et al. (1999) in their laboratory study found

$$[C_2H_3CN]_{\text{upper limit}}/[HCN]_{\text{upper limit}} = 1.3 \times 10^{-3},$$

much smaller than the order of magnitude factor found in the lower stratosphere by comparing Figs. 3 and 5a. A large C_2H_3CN density results in C_2H_3CN photolysis as the main source of HC_3N, and thus, the cause of this apparent overprediction needs to be analyzed. Considering that the synthetic profiles of C_2H_2 and HCN match observations in the stratosphere, the most likely causes of this large prediction are: (1) underconsideration of acrylonitrile loss, (2) incorrect chemical mechanism regarding the formation of C_2H_3CN or (3) other considerations affecting C_2H_3CN loss.

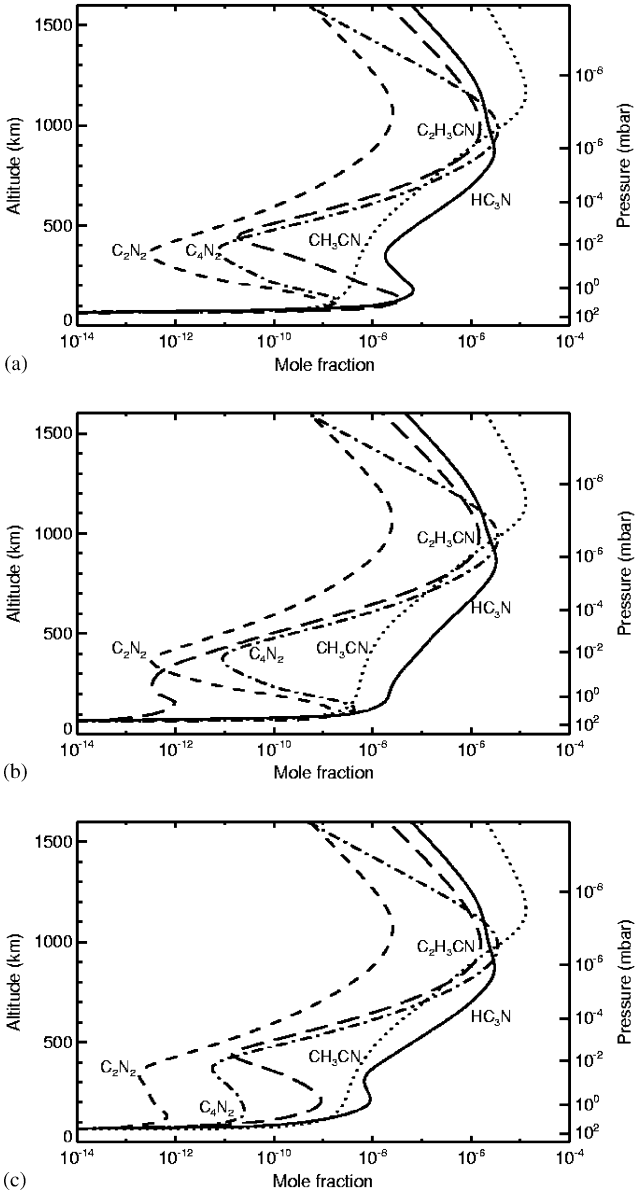

Fig. 5. (a) Abundance profiles for key nitrile species, assuming fractal haze opacities and the Monks et al. (1993) rate coefficient for $HCN + C_2H_3$. (b) Nitrile abundance profiles calculated neglecting $HCN + C_2H_3$. (c) Nitrile abundance profiles assuming Mie haze opacities.

Scenario (1) *not enough C_2H_3CN loss is being considered*: The photodissociation of C_2H_3CN is modeled using the unpublished data of F. Raulin (pers. comm.), with the

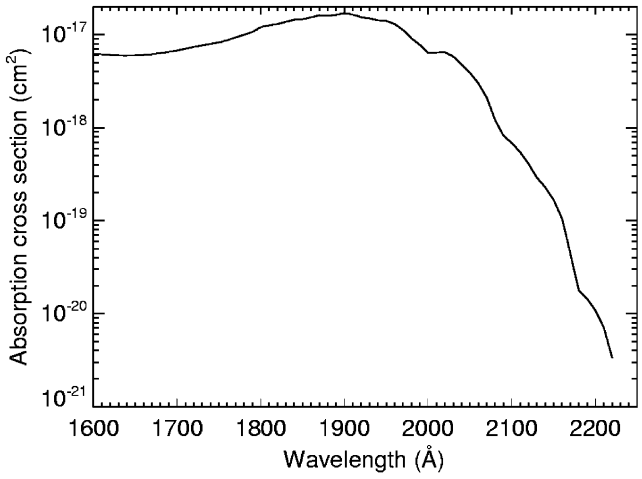

Fig. 6. Absorption cross section for C_2H_3CN (F. Raulin, pers. comm.).

cross section shown in Fig. 6. This C_2H_3CN cross section, larger than assumptions made previously (Toublanc et al., 1995) allows photolysis to be easily the dominant loss mechanism for stratospheric C_2H_3CN, through which cyanoacetylene is the primary benefactor (Derecskei-Kovacs and North, 1999). If underconsideration of acrylonitrile photolysis were the main cause of C_2H_3CN overprediction, this cross section would have to be significantly larger. However, considering its broad continuum nature and its extent into the NUV, particularly in the context of other nitrile spectra, it is difficult to image a larger cross section to the extent of significantly reducing the C_2H_3CN stratospheric mole fraction by orders of magnitude. Furthermore, such a cross section would result in a larger HC_3N modeled abundance, which is already too high compared to observations. Other mechanisms involving C_2H_3CN destruction which are not considered in the model may be taking place, but such a mechanism efficient enough to overwhelm photolysis in the stratosphere is unlikely, especially considering photolysis dominates the loss of all known large stable nitrile molecules in Titan's stratosphere. For these reasons, this scenario is removed from consideration.

Scenario (2) *faulty chemical mechanisms regarding acrylonitrile production*: The large densities of HCN and C_2H_2 along with the pressure-induced hydrogen attachment onto acetylene allow (S6) to be very efficient in producing C_2H_3CN, despite the small rate coefficient of the producing reaction ($k = 2.7 \times 10^{-15}$ cm^3 s^{-1}@150 K). This reaction, measured by Monks et al. (1993), did not produce a definitive yield in the laboratory as only trace amounts of C_2H_3CN were identified in the experiment. Monks et al. assumed addition–decomposition as the favored mechanism of C_2H_3 + HCN through analogy with HCN + C_2H and C_2H_2 + C_2H. However, the hypothesis that C_2H_3CN production through this mechanism may be significantly smaller than assumed remains a real possibility.

Scenario (3) *other considerations affecting C_2H_3CN loss*: The acrylonitrile cross section extends into the 1800–2200 Å region, where haze particles provide the dominant opacity (McGrath et al., 1998). Titan haze opacity, however, is still a pressing issue. Microphysical models have attempted to describe the nature of Titan haze and its opacity. Models such as Toon et al. (1992) and McKay et al. (1989) have used Mie scatterers as analogues for Titan haze particles while fractal models (e.g. Cabane et al., 1993), Rannou et al., 1995, 1997) have simulated Titan haze using fluffy aggregates of monomers. Spherical Mie models have been able to reproduce the observed geometric albedo, while until recently (Rannou and McKay, 2003), fractal models have had difficulty matching the methane feature at 0.64 μm. However, photometric and polarimetric data have suggested that Titan haze does take the form of fluffy fractal aggregates. Fractal particles are more opaque than Mie particles at short wavelengths (Rannou et al., 1995), affecting the radiation available to photolyze constituents in the stratosphere. Most affected are constituents that primarily absorb at wavelengths larger than 1800 Å, like C_2H_3CN. However, as Titan aerosol densities and optical constants are still not well understood, aerosol opacities provide a significant uncertainty for photodissociation coefficients of affecting constituents.

To test scenarios (2) and (3), sensitivity studies are conducted, considering a case where the reaction HCN+C_2H_3 is omitted and a case using Mie opacities derived from Rannou et al. (1995) as opposed to the nominal case which uses fractal opacities from Rannou et al. (1995) and Lebonnois et al. (2001). Fig. 5b shows that the omission of the HCN + C_2H_3 source decreases the acrylonitrile abundance in the lower stratosphere by more than four orders of magnitude. The corresponding change in HC_3N results in a reduction of a factor of three at 105 km. In the Mie example (Fig. 5c), the mole fractions of all of the large nitrile molecules are significantly reduced in the lower stratosphere, with the exception of CH_3CN, which does not significantly absorb longward of 1800 Å (Suto and Lee, 1985). The value of 5.3×10^{-10} for the HC_3N mole fraction in the Mie case agrees with the ISO disk-averaged value obtained with a HC_3N contribution peak at $\sim$ 105 km (Coustenis et al., 2003). Marten et al. (2002) millimeter observations retrieved much lower abundances for HC_3N in the region of the atmosphere, although the shape of their HC_3N profile in the lower stratosphere sharply differs from photochemical models.

It is unclear which of these causes is responsible for the large HC_3N and C_2H_3CN densities found in Fig. 5a or to what degree both are responsible. Thus, in order to obtain more likely abundances for the purpose of estimating yields of various haze-forming mechanisms, k(HCN + C_2H_3) is reduced by a factor of 10^{-3}, with the results shown in Fig. 7a. Note that the densities for HC_3N and C_4N_2 in this nominal case are most likely still too high in the lower stratosphere, with a HC_3N mole fraction of 4.4×10^{-9} at 105 km.

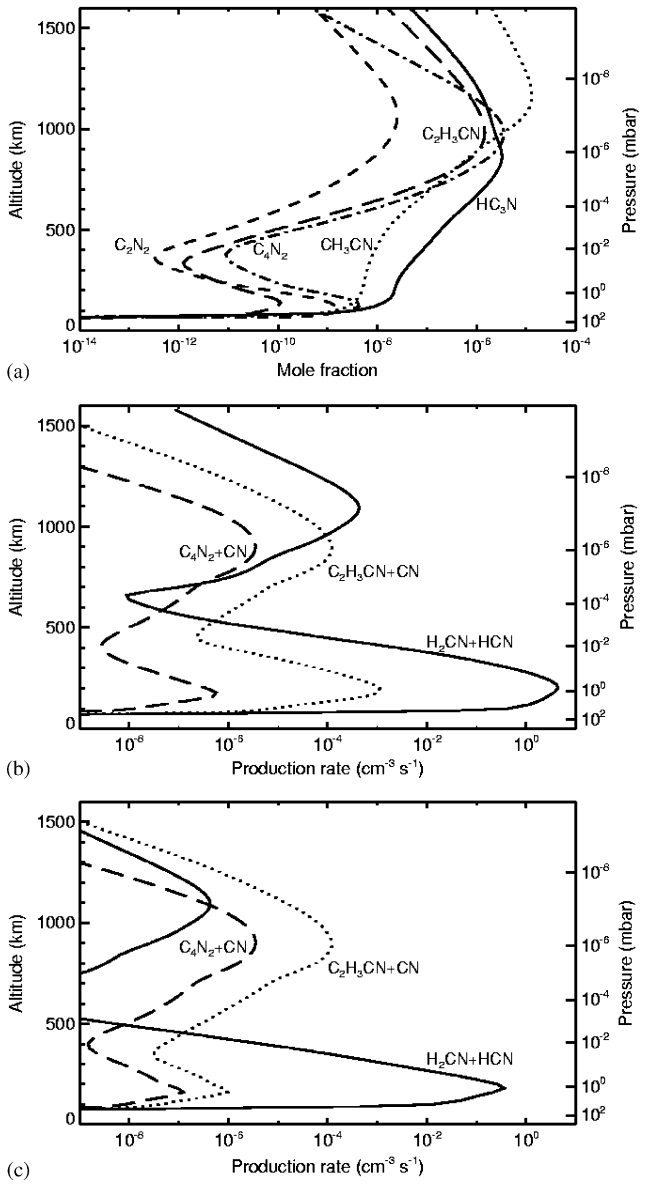

Fig. 7. (a) Nominal abundance profiles for key nitrile species assuming $k(\mathrm{HCN} + \mathrm{C_2H_3}) = 10^{-3} \times k$ (Monks et al., 1993). (b) Production rate profiles for nitrile-pathway haze production mechanisms, assuming $k(\mathrm{HCN} + \mathrm{C_2H_3}) = k$ (Monks et al., 1993). (c) Production rate profiles for nitrile-pathway haze production mechanisms, assuming $k(\mathrm{HCN} + \mathrm{C_2H_3}) = 10^{-3} \times k$ (Monks et al., 1993).

3.2. Haze pathways

To account for polymerization through CN-insertion, the pure nitrile pathway (NT-polymer) to haze formation is assumed to follow via the addition of CN to high-order nitriles:

$$\mathrm{CN} + \mathrm{C_2N_2} \rightarrow \text{NT-polymer}, \quad \text{(R16)}$$

$$\mathrm{CN} + \mathrm{C_2H_3CN} \rightarrow \text{NT-polymer}, \quad \text{(R17)}$$

$$\mathrm{CN} + \mathrm{C_4N_2} \rightarrow \text{NT-polymer}. \quad \text{(R18)}$$

In accordance with Thompson and Sagan (1989), the reaction of H_2CN with HCN is proposed to contribute to the formation of long-chain nitriles in the path towards polymerization:

$$\mathrm{H_2CN} + \mathrm{HCN} \rightarrow \text{NT-polymer}. \quad \text{(R19)}$$

(R19) has not been kinetically studied so we assume a rate coefficient equal to that of $k(\mathrm{HCN} + \mathrm{C_2H_3})$, a rate coefficient also considered in Lebonnois et al. (2002) for this reaction. The evidence for kinetically similar behavior for H_2CN and C_2H_3 is that rate coefficients for $H_2CN + H$ and $H_2CN + N$ (Nesbitt et al., 1990) are within a factor of two of the rate coefficients for $C_2H_3 + H$ (Monks et al., 1995) and $C_2H_3 + N$ (Payne et al., 1996), respectively. However, this assumption must be taken under advisement as HCN does not proceed very quickly through reaction with other nitriles. Stable–RCN molecules (e.g. CH_3CN) will most likely proceed very slowly, if at all, with HCN. Fig. 7b shows the polymer production from (R16)–(R19), assuming the Monks et al. (1993) rate for $HCN + C_2H_3$ and (R19), while Fig. 7c shows the production rates from the different nitrile mechanisms assuming the reduced Monks et al. rate. It is clear that nitrile-produced haze is triggered by (R19) in the lower stratosphere in both cases. At higher altitudes, polymer is generated through the CN-insertion mechanism.

4. PAH polymers

Polymerization of acetylene can also result in the formation of Polycyclic Aromatic Hydrocarbons (PAHs), which can be found in circumstellar nebulae and interplanetary dust particles (Clemett et al., 1994; Buss et al., 1993), and are believed to exist prominently in the interstellar medium (Allamandola et al., 1989). Although most studies regarding PAHs involve high temperature combustion conditions, PAHs have been identified in laboratory simulations of Jupiter and Titan haze (Sagan et al., 1993). Furthermore, the detection of benzene (C_6H_6), the simplest of aromatic hydrocarbons, on Jupiter and Saturn (Bézard et al., 2001), the tentative detection of benzene on Titan (Coustenis et al., 2003), and identification of benzene in laboratory simulations of Titan's atmosphere (Coll et al., 1999) together suggest that PAH synthesis proceeds in planetary atmospheres, as well.

Benzene is formed in the atmosphere of Titan primarily through the pressure-induced recombination of propargyl radicals (Wilson et al., 2003). Once the closure of that first aromatic ring has occurred, leading to the establishment of the benzene molecule or its hydrogen-abstracted radical equivalent, phenyl (C_6H_5), the propagation of PAH formation is promoted through the

attachment of ethynyl radical onto benzene or acetylene onto phenyl:

$$C_6H_5 + C_2H_2 \rightarrow \text{PAH-polymer}, \quad \text{(R20)}$$

$$C_6H_5 + C_2H_2 \rightarrow \text{PAH-polymer}. \quad \text{(R21)}$$

This mechanism, known as the HACA (H-abstraction/C_2H_2-addition) sequence, may proceed through continued H-abstraction followed by acetylene addition as proposed by Wang and Frenklach (1997) or through continued acetylene-addition to close the second ring as proposed by Bittner and Howard (1981). These mechanisms, forming the two-ring naphthalene are illustrated in Fig. 8. The Bittner-Howard version appears to be more important at low temperatures (Bauschlicher Jr. and Ricca, 2000), providing the basis for the formation of the PAH-polymer.

Wilson et al. (2001) and Wilson (2002) consider the HACA mechanism as the primary source of polymerization through aromatic chemistry. Assuming that PAH production beyond the first aromatic ring goes into Titan haze, the reactions to consider for PAH-polymer formation are (R20) and (R21), which were also considered by Lebonnois et al. (2002), along with

$$C_6H_6 + C_6H_5 \rightarrow \text{PAH-polymer} \quad \text{(R22)}$$

with k(R20) and k(R21) taken from the Wang and Frenklach (1997) measurements and k(R22) from Park et al. (1999).

Wilson et al. (2003) suggest the possibility of benzene formation in Titan's atmosphere, corroborated by the tentative detection of benzene by ISO (Coustenis et al., 2003). The observation fit by a uniform mole fraction profile of $4 \pm 3 \times 10^{-10}$ was matched by a vertical profile of benzene from Wilson et al. (2003), multiplied by 3.0 ± 0.5, an upper-limit profile calculated assuming reaction rates for aromatic compounds that correspond to a temperature of 300 K. However, aerosol opacity was not considered in that calculation. Haze particles act to shield benzene from photodissociation, which extends as far as 2700 Å (Pantos et al., 1978). Fig. 9a shows the benzene photodissociation coefficient calculated for the Wilson et al. (2003) profile compared with that under fractal and Mie opacities, and the corresponding benzene profiles are shown in Fig. 9b. The updated benzene profiles, including NUV shielding by haze particles and calculated with the nominal Titan temperature profile (Yelle et al., 1997), are found to be consistent with the ISO tentative detection in Titan's stratosphere, with the fractal profile at the upper end of the constraint and the Mie profile tapering off below 200 km. The larger abundance of C_6H_6 in the upper atmosphere for the Wilson et al. profile is due to the larger rates corresponding with the 300 K assumption described above.

Wang and Frenklach (1994, 1997) measured rates of reaction for (R20) and (R21) for minimum temperatures varying from 300 to 500 K, with the temperature range extending up to 2500 K. This presents some difficulties when extrapolating down to Titan-like temperatures. Yu et al. (1994) obtained a rate expression for (R21) for the temperature range of 297–523 K. This rate is compared with the Wang and Frenklach rate, assuming high-pressure conditions, in Fig. 10a. In Titan's temperature regime, Yu et al. rate exceeds the Wang and Frenklach rate by as much as two orders of magnitude. Yu et al. rate is adopted as the study is more focused on the low temperature regime. However, this discrepancy highlights the need for more low temperature kinetic measurements of aromatic chemistry.

The impact of the two rates for (R21) on the benzene profile is shown in Fig. 10b. The pathway to polymerization is not the main loss mechanism for benzene, but rather photolysis. Thus, the enhanced loss from the Yu et al. rate results in only a 20% depletion in benzene density over what is found using the Wang and Frenklach rate. However, as Fig. 10c highlights, the increased rate results in an order of magnitude increase in polymer production in the lower stratosphere, with the peak of production rising from 180 to 220 km. In this profile, (R21) is clearly the dominating PAH-polymer mechanism at the peak of production, due to the involvement of the abundant acetylene molecule. At this altitude, (R20) and (R22) are four and five orders of magnitude less efficient, respectively. Above 400 km, (R20) is the dominant PAH-polymer producing mechanism.

A possible pathway to haze is polymerization through the aliphatic version of C_6H_5. Lebonnois et al. (2002) considered a path to haze formation through the reaction of the linear n-C_6H_5 with C_2H_2. The reaction kinetics involving the n-C_6H_5 molecule, however, have not been adequately studied in the laboratory to provide much guidance as to its kinetic behavior. Wang and Frenklach (1997), examining n-$C_6H_5 + H$, assume a rate coefficient for the addition mechanism to be equal to $C_4H_3 + H$ while the hydrogen abstraction pathway is assumed at $0.5 \times k(C_2H_3 + H)$, which in the case of C_2H_2 would be an order of magnitude smaller than reaction with C_4H_3, assuming the Wang and Frenklach rates. In addition to the ambiguity of what is the proper proxy for n-$C_6H_5 + C_2H_2$, there is large disagreement regarding the reaction rate of $C_4H_3 + C_2H_2$ at low temperatures. Extrapolation of the highly pressure-dependent $C_4H_3 + C_2H_2$ rate coefficient using the Wang and Frenklach (1994) expressions yields a rate coefficient of 4.8×10^{-18} cm^3 s^{-1} for $T = 170$ K, $p = 1$ mbar, for the n-C_6H_5 pathway. However, an extrapolation of the Westmoreland et al. rate (1989) yields a $C_4H_3 + C_2H_2 \rightarrow n$-$C_6H_5$ rate coefficient of 1.7×10^{-20} cm^3 s^{-1} for $T = 170$ K, $p = 1$ mbar.

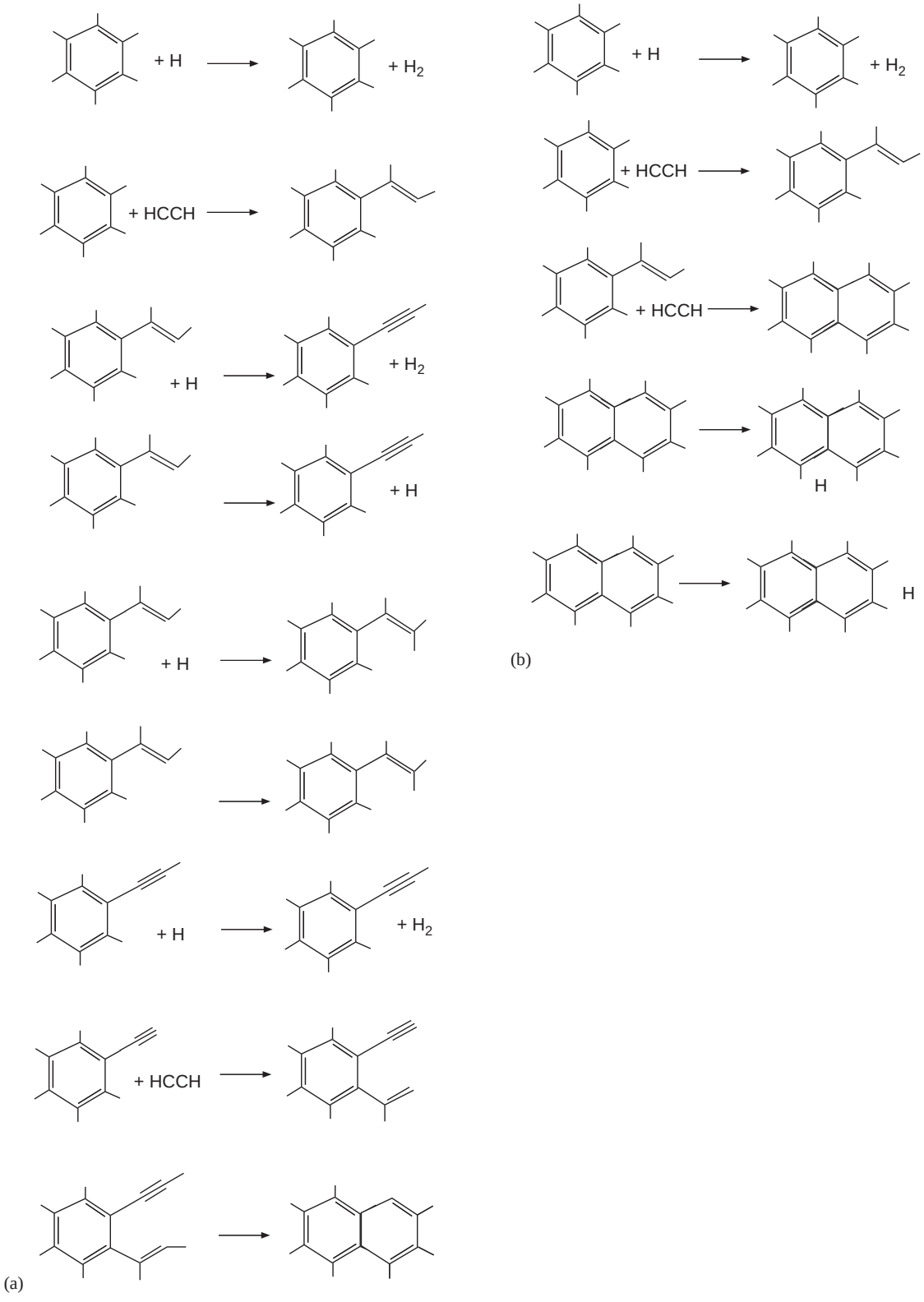

Fig. 8. Mechanisms of PAH formation proposed by (a) Frenklach et al. and (b) Bittner and Howard. (after Bauschlicher and Ricca, 2000).

Such a reduction in rate coefficient translates to a haze precursor rate of 1.4×10^5 cm^{-2} s^{-1} from this pathway as opposed to 7.0×10^6 cm^{-2} s^{-1} assuming the Wang and Frenklach rates. The linear version of this molecule may also collisionally isomerize to phenyl, which has a much lower ground-state energy (Westmoreland

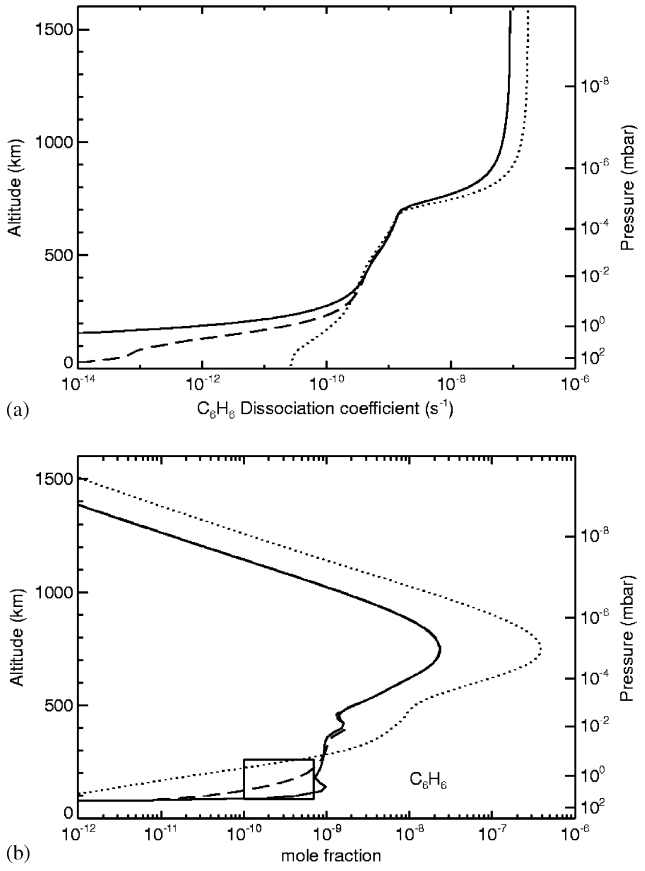

Fig. 9. (a) Benzene photodissociation coefficient assuming fractal haze particles (solid line), Mie particles (dashed line), and no haze (dotted line) used in Wilson et al. (2003). (b) Benzene profiles assuming fractal haze particles (solid line) and Mie particles (dashed line). The benzene profile from Wilson et al. (2003) (dotted line) is included. The rectangle represents the ISO detection of benzene (Coustenis et al., 2003).

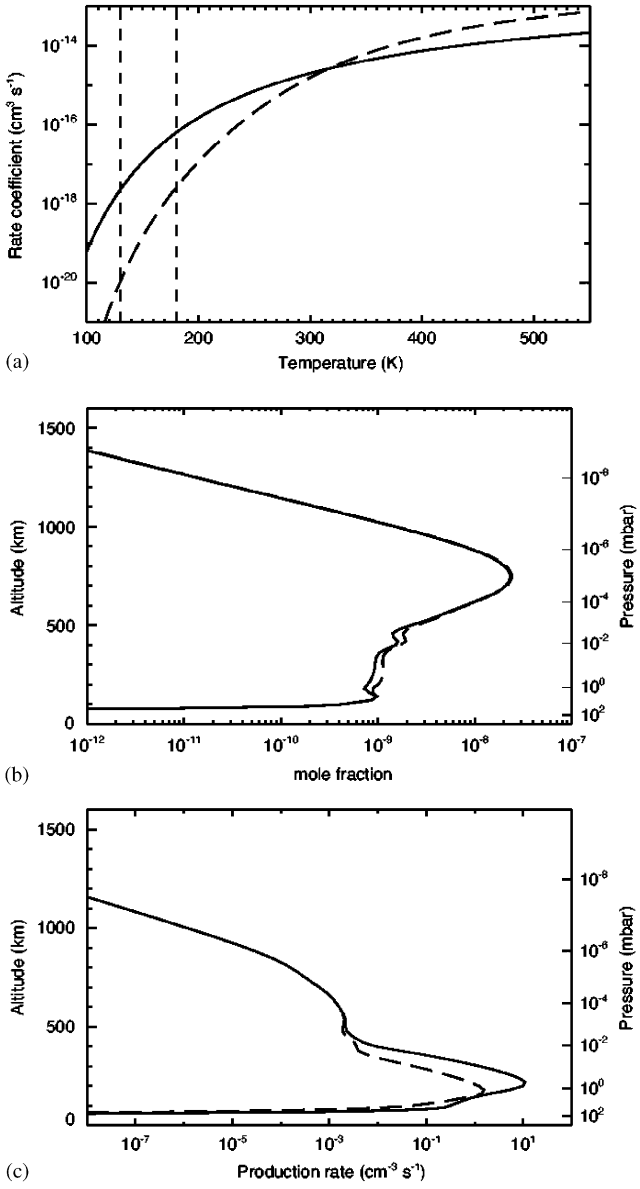

Fig. 10. (a) Rate coefficient for $C_6H_5 + C_2H$ from Yu et al. (1994) (solid line) and Wang and Frenklach (1994) (long-dashed line). Short-dashed line represents the boundaries of the temperature region in which significant Titan chemistry takes place. (b) Benzene abundance profile, assuming for the $C_6H_5 + C_2H$ rate Yu et al. (1994) (solid line) and Wang and Frenklach (1994) (long-dashed line). (c) Production rate profiles for aromatic-pathway haze production mechanisms, assuming $k(C_6H_5 + C_2H) = k$ (Yu et al., 1994) (solid line) and $k(C_6H_5 + C_2H) = k$(Wang and Frenklach, 1994) (long-dashed line).

et al., 1989), enhancing the aromatic contribution to haze.

5. Copolymers

As hydrocarbons and nitriles react with each other in Titan's atmosphere, there is a likelihood that Titan's haze particles are, at least in part, the products of such chemical mixing. Copolymerization of hydrocarbon and nitrile mixtures has been identified in laboratory simulations as exhibiting optical properties that are comparable to Titan haze (Bar-Nun et al., 1988; Clarke and Ferris, 1996).

5.1. Aliphatic copolymers

With HC_3N much more reactive in the gas phase than HCN, cyanoacetylene presents a good case as a candidate for polymerization. Laboratory studies have shown that HC_3N polymerizes much faster than HCN (Scattergood et al., 1992) and is 2–5 times more reactive in polymer formation than C_2H_2 (Clarke and Ferris, 1996). Laboratory studies indicate that gas-phase aromatic compounds 1,2,4- and 1.3.5-tricyanobenzene result from photolysis of HC_3N at low temperatures, with polymer as the major photoproduct (Ferris and Guillemin, 1990).

Clarke and Ferris (1997) have studied polymers arising from the irradiation of mixtures of HC_3N and various hydrocarbons (C_2H_2, C_2H_6, n-C_4H_{10}). They suggest

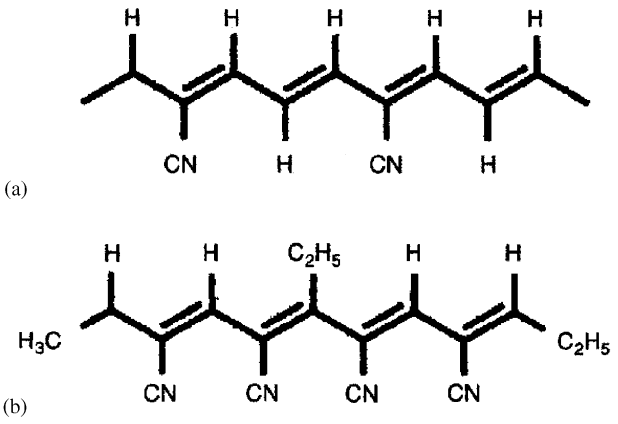

Fig. 11. Possible structures for HC_3N polymers incorporating (a) C_2H_2 and (b) C_2H_6. (After Clarke and Ferris, 1997, Icarus, 127, 158–172).

incorporation of C_2H_5 radicals in the HC_3N/C_2H_6 polymer and the formation of a copolymer resulting from the irradiation of the HC_3N/C_2H_2 mixture, with the possible structures shown in Fig. 11.

In the lower atmosphere, acetylene and ethane undergo photolysis and pressure-induced hydrogen addition to form the more highly reactive C_2H, C_2H_3, and C_2H_5. To examine the possibilities of haze formation from copolymerization of HC_3N with acetylene and ethane, the following reactions are considered for the initiation of copolymerization:

$$HC_3N + C_2H \rightarrow \text{products}, \quad (R23)$$

$$HC_3N + C_2H_3 \rightarrow \text{products}, \quad (R24)$$

$$HC_3N + C_2H_5 \rightarrow \text{products}. \quad (R25)$$

HC_3N has many similarities with C_2H_2, structurally and photolytically (Clarke and Ferris, 1996). HC_3N absorbs UV light in the wavelength region of 1060–2600 Å and yields photoproducts through three pathways:

$$HC_3N + h\nu \rightarrow CN + C_2H, \quad (R26)$$

$$HC_3N + h\nu \rightarrow C_3N + H, \quad (R27)$$

$$HC_3N + h\nu \rightarrow HC_3N^*. \quad (R28)$$

The quantum yields for these three pathways are 0.05, 0.09, and 0.86, respectively (Clarke and Ferris, 1995; Halpern et al., 1988). The evidence that HC_3N kinetically behaves in a similar fashion is, admittedly, rather sparse, largely due to the few studies exploring the kinetics of reactions involving HC_3N. Yung (1987) estimated the hydrogen addition to HC_3N to proceed with a rate coefficient equal to $C_2H_2 + H$. In CN-insertion reactions, Halpern et al. (1989) measured a rate coefficient for $CN + HC_3N$ that is an order of magnitude lower than that for $CN + C_2H_2$ (Sims et al., 1993) at the same temperature. Nevertheless, in an attempt to derive an upper limit for possible mechanisms responsible for copolymerization, rate coefficients for (R23)–(R25) are taken from $C_2H_2 + C_2H$ (Chastaing et al., 1998), $C_2H_2 + C_2H_3$ (Weissmann and Benson, 1988), and $C_2H_2 + C_2H_5$ (Kerr and Parsonage, 1972), respectively. Assuming these rates, (R23) is the dominant producer at all altitudes among these reactions, with (R24) an order of magnitude smaller in the lower stratosphere.

However, the question remains whether (R23) represents the initiation of a process that will result in sufficient polymerization. Lebonnois et al. (2002) considered this reaction in a polymer-producing scheme, assuming cyanodiacetylene (HC_5N) to be the product of a C_2H-insertion-H-abstraction mechanism. Such a mechanism, along with CN-insertion-H-abstraction (Seki et al., 1996), may be responsible for the formation of such unsaturated cyanopolyynes as HC_5N and HC_7N, which have been identified in interstellar molecular clouds (Winnewisser and Walmsley, 1978). Lebonnois et al. (2002) also considered the involvement of the cyanoethynyl radical (C_3N) in the formation of HC_5N. Assuming C_3N to proceed kinetically at a rate similar to CN and HC_5N to photodissociate in a similar manner as HC_3N yields a HC_5N mole fraction of 8.5×10^{-10} at 105 km, with $C_3N + C_2H_2$ acting as the primary source of cyanodiacetylene. Little attention has been given to kinetic processes involving the cyanoethynyl radical, other than estimates from Yung (1987) regarding recycling processes back to HC_3N. Furthermore, the photodissociation dynamics of HC_5N has not been studied. Nevertheless, laboratory detection of HC_5N suggest much smaller abundances, with de Vanssay et al. (1995) estimating a value for HC_5N of 10^{-2} times that for HC_3N, while Coll et al. (1999) find the HC_5N mole fraction within a range of $1.3–6.4 \times 10^{-13}$. Moreover, Marten et al. (2002) place an observational upper limit of 4×10^{-10} above 80 km. Considering the unlikelihood of major differences between HC_3N and HC_5N photolysis, these results suggest that the larger C_3N radical might react with hydrocarbons at a significantly lower rate than CN. The omission of $C_3N + C_2H_2$ yields a HC_5N mole fraction of 9.6×10^{-12} at 105 km.

The laboratory and observational non-detection of HC_5N also suggest a pattern that is illustrated in the analysis of polyacetylenes, shown in Section 2. Largely due to the small yields for radicals responsible for the propagation of chemistry (e.g. CN, C_2H), the abundances of $HC_{2n+1}N$ cyanopolyynes appear to drop off on a similar scale as $C_{2n}H_2$ polyynes as n increases, a drop-off on the order of 10^{-2}–10^{-3} at each level. As demonstrated for polyacetylenes in Section 2, such a drop off does not bode well for the production of haze from such a mechanism. Any other chemical mechanisms involving HC_5N loss, such as hydrogen addition considered by Lebonnois et al. (2002), will be minor compared to photolysis and will produce a compound with an abundance too small to significantly contribute to haze formation. On the other hand, the diminution of the C_3N radical as a consideration and the large yield for HC_3N^*

from cyanoacetylene photolysis raise the possibility of the metastable state as a viable pathway towards substantial polymerization.

Both acetylene and diacetylene have dissociation pathways that primarily yield the metastable state (Seki and Okabe, 1993; Glicker and Okabe, 1987). At 193 nm, metastable acetylene ($C_2H_2^*$) reacts with the ground state to produce diacetylene at a faster rate than quenching (Seki et al., 1986). Furthermore, as stated earlier, the reaction of $C_4H_2^*$ with C_4H_2 (Bandy et al., 1993) is responsible for much of the C_8H_2 formed in Titan's atmosphere, as well as reaction with acetylene (Frost et al., 1996) acting as a primary contributor to the formation of C_6H_2.

Clarke and Ferris (1996) measured significant consumption of HC_3N compared to C_2H_2 in the irradiation of C_2H_2/HC_3N mixture at 185 nm in the presence of N_2. Considering the significant loss of HC_3N of polymerization and the large photolytic yield of HC_3N^*, underlining the role the metastable state might play in polymer formation, a reaction involving HC_3N^* and C_2H_2 is considered as a pathway to polymerization

$$HC_3N^* + C_2H_2 \rightarrow \text{Co-Polymer}, \quad \text{(R29)}$$

resulting in a copolymer similar to the structure shown in Fig. 11a. The rate coefficient for this reaction is taken from $C_4H_2^* + C_2H_2$ (Frost et al., 1996). The deexcitation of HC_3N^* is taken to be equal to the $C_4H_2^*$ deexcitation rate (Zwier and Allen, 1996).

5.2. Aromatic copolymers

Ricca et al. (2001) analyzed mechanisms involving the incorporation of nitrogen into an aromatic molecule as a source of Titan haze. A possible mechanism included a Bittner-Howard-like scheme, commencing with H-abstraction from pyridine (C_5H_5N). However, the mechanism by which pyridine is formed on Titan is unclear. The reaction $C_5H_6 + N \rightarrow C_5H_5N + NH$ is exothermic by 95 kJ/mol, but C_5H_6 formation is largely inhibited on Titan, due to the large activation energy of $C_3H_5 + C_2H_2 \rightarrow C_5H_6 + H$ (Burcat and Dvinyaninov, 1997). C_4H_5-insertion into HCN is thermodynamically feasible,

$$C_4H_5 + HCN \rightarrow C_5H_5N + H,$$
$$\Delta H_f^0 = -122 \text{ kJ/mol}. \quad \text{(R30)}$$

However, assuming (R30) to proceed in a similar fashion as $HCN + C_2H_3$ renders (R30) a relatively minor pathway to polymer formation.

Another mechanism suggested by Ricca et al. (2001) involves the adding of HC_3N to the phenyl radical,

$$C_6H_5 + HC_3N \rightarrow \text{Co-polymer}, \quad \text{(R31)}$$

in a similar manner as (R21). Assuming the rate coefficient to be equal to k(R21), this mechanism produces haze precursors at a similar rate as the aliphatic copolymer mechanisms.

6. Discussion

Haze particles are the product of the growth of gas-phase molecules which reach a stage of particle inception. At this stage, these molecular precursors of the haze begin to nucleate, which facilitates the conversion from gas-phase to particulate form. In the case of PAHs, this nucleation begins around 2000 amu (Richter and Howard, 2000), which would require an aggregation on the order of about 20 molecules in the haze precursor, assuming each of the molecules to have the total mass of the reactants in the primary reaction (Table 2). As this process is still poorly understood, regardless of temperature or chemical composition, it is assumed that all precursor pathways nucleate at the 20 molecule level. Assuming that as the precursor grows, any loss due to chemistry is negligible, Wilson and Atreya (2001) and Wilson (2002) obtain a haze column production rate by multiplying the precursor production rate by the nucleation mass. This methodology differs from that of Lebonnois et al. (2002), which propose that the aggregation of 10–100($\sim$ 20) parent molecules preceed the nucleation of the macromolecule, wich is on the order of 600 amu. Using our methodology, the model calculates haze column production rates for the various mechanisms shown in Table 2. The nominal case yields a haze production rate of 3.2×10^{-14} g cm^{-2} s^{-1}, a little larger than what is suggested by the microphysical models. This result is considered an upper limit for the mechanisms considered, as loss of precursors due to chemistry, dynamics, and condensation will most certainly reduce the haze production rate (Wilson, 2002). This haze production rate derives primarily from the PAH pathway. There is a significant nitrile component in the lower stratosphere (Fig. 12), which makes up about 40% of the haze at 1 mbar and approximates the aromatic contribution below 180 km. However, the PAH pathway dominates haze production throughout much of the lower atmosphere. Above 800 km, nitriles take over haze formation, peaking at 850 km, near the source region suggested by Chassefière and Cabane (1995). This upper atmosphere source may contribute to the detached haze layer that presides at higher altitudes, although there may be an additional source from below, which becomes detached as a result of dynamical processes (Rannou et al., 2002). Copolymers, for the most part, provide a minor source for Titan haze, according to this calculation, while polyynes demonstrate a negligible effect.

This result for the total haze production rate agrees with the value obtained by Lebonnois et al. (2002) of 4.1 $\times$

Table 2
Column production rates for the various haze sources

		Primary reaction	Precursor production rate (cm^{-2} s^{-1})	Haze production rate (g cm^{-2} s^{-1})
Pure polyyne	PA-Polymer	$C_6H_2 + C_4H$	8.7×10^2	3.6×10^{-18}
Pure nitrile	NT-Polymer	$H_2CN + HCN$	2.4×10^6	4.4×10^{-15}
PAH	PAH	$C_6H_5 + C_2H_2$	9.5×10^6	3.2×10^{-14}
Aromatic copolymer	Co-Polymer	$C_6H_5 + HC_3N$	2.4×10^5	1.0×10^{-15}
Aliphatic copolymer		$HC_3N^* + C_2H_2$	1.2×10^5	3.0×10^{-16}

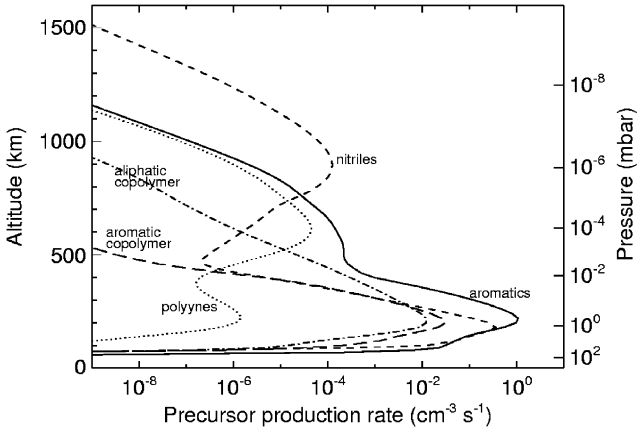

Fig. 12. Total haze production rate profiles for the pure polyyne, pure nitrile, pure aromatic, aromatic copolymer, and aliphatic copolymer pathways.

10^{-14} g cm^{-2} s^{-1}, which peaks at a slightly lower level around 170 km. However, the sources responsible for the haze differ between the two models. While the nominal model attributes haze production largely a result of PAH growth, Lebonnois et al. derive a PAH source approximately four orders of magnitude smaller. The main cause of this difference is the small abundance of benzene in their study (Lebonnois et al., 2002, Fig. 3), 3–4 orders of magnitude smaller than the nominal stratospheric abundance and ISO observation (Coustenis et al., 2003). Lebonnois et al. find acetylene polymers and HC_3N/C_2H_2 copolymers to be mainly responsible for haze production, based largely on a value for the rate coefficient of $C_4H_3 + C_2H_2 \rightarrow n\text{-}C_6H_5$ of 2×10^{-16} cm^3 s^{-1}, attributed to Wang and Frenklach (1994). However, considering the temperature range in the region of their maximum haze formation and the Wang and Frenklach high-pressure temperature-dependent expression, this rate coefficient can be reduced by as much as a factor of 3.5. Furthermore, it is clear by Wang and Frenklach, 1994, 1998 and Westmoreland et al. (1989) studies that this reaction has a significant pressure-dependence, which is not considered in the Lebonnois et al. study. There are also differences between the Wang and Frenklach and Westmoreland et al. rate coefficients, which are discussed in Section 2. The larger rate from HC_3N/C_2H_2 copolymers in Lebonnois et al. (2002) is also enhanced by their HC_3N profile, which is at least an order of magnitude too high in the lower stratosphere, based on observations (Coustenis et al., 1989; Marten et al., 2002) and laboratory simulations (Coll et al., 1999), although the low C_4H_2CN density that is hinted at in Lebonnois et al. suggests that HC_3N does not play a significant role in copolymerization with acetylene. The nitrile component to the haze in the nominal model agrees with Lebonnois et al. in the lower stratosphere, with the difference in the haze production rate for this pathway due more to the way the haze production rate is calculated, rather the chemical output.

Of course, there are a number of uncertainties inherent in this study. For instance, assuming the Monks et al. (1993) rate is appropriate for both $HCN + C_2H_3$ and $HCN + H_2CN$, providing large stratospheric densities for HC_3N and C_2H_3CN, nitriles can be responsible for as much as 9.2×10^{-14} g cm^{-2} s^{-1} of haze production, due to the larger rate coefficient, an aspect illustrated in the comparison of Figs. 7b and c. The aliphatic copolymer mechanism provides a minor source for the haze from the $HC_3N^* + C_2H_2$ reaction, assuming HC_3N^* quenches at a similar rate as $C_4H_2^*$. However, the high rate of HC_3N polymerization (Scattergood et al., 1992; Clarke and Ferris, 1996) as compared to acetylene may signal that the metastable variety does not quench as quickly as acetylene or diacetylene. 10% of the HC_3N^* quenching rate going toward polymerization would result in a precursor production rate of 1.0×10^7 cm^{-2} s^{-1}. Furthermore, more study into the kinetic behavior of C_4H_3 and $n\text{-}C_6H_5$ molecules would provide better insight into the contribution of copolymers and aliphatic hydrocarbons to Titan haze. This highlights the necessity for more kinetic study on these reactions at low temperature, as well as the photochemical trail of molecules like HC_3N^*, which may play a significant role in haze formation. In addition, this study underlines the potential importance of aromatic molecules, whose mechanisms, in particular $C_6H_5 + C_2H_2$, need to be analyzed at temperatures applicable to outer planetary atmospheres.

Laboratory simulations of Titan haze production have attempted to identify the composition of Titan haze through tholin analysis. Electrical discharge experiments have measured simulated tholin to have a C/N ratio of 1.9–11 and a H/C ratio near unity (McKay et al. 2001, and all refer-

ences within), suggesting a larger contribution from nitrogen compounds than what is found in this study. These experiments simulate the influence that precipitating electrons and UV radiation below 1000 Å have on Titan's atmospheric chemistry, but do not well describe the impact of UV radiation longer than 1000 Å (Tran et al., 2003). The former is responsible for dissociation of nitrogen molecules, which are essential in the formation of nitriles, while radiation longer than 1000 Å help propagate hydrocarbon chemistry. This characteristic of discharge experiments is illustrated in the plasma discharge experiments of Coll et al. (1999). In these experiments, a C/N ratio of 2.82 was found for the simulated tholin, while 70 organic compounds were detected. In comparison with observations, the HCN and HC_3N output found good agreement. However, the hydrocarbons, with the exception of methylacetylene, were consistently underrepresented. Tran et al. (2003) conducted laboratory simulations using a photochemical flow reactor and a gas mixture containing Titan atmospheric constituents that may be important in polymerization. In these experiments, they found a polymeric product with a C/N ratio of 17.6, much higher than the discharge experiments. It should be noted that these experiments were conducted assuming a HC_3N/C_2H_2 ratio of 5.0×10^{-2}, consistent with the IRIS north pole observations (Coustenis et al., 1991) while much larger than the ISO disk-averaged observations that derive a HC_3N/C_2H_2 ratio of 9.0×10^{-5} (Coustenis et al., 2003). The experimental HC_3N/C_2H_2 ratio is consistent with ISO disk-averaged ratio of HCN/C_2H_2 (5.4×10^{-2}), and HC_3N polymerizes much faster than HCN (Scattergood et al., 1992), which suggests that the experimental C/N ratio found by Tran et al. may be a lower limit.

Microphysical models, assuming a more simplistic haze production rate profile, have used laboratory-generated tholin to fit Titan's geometric albedo, obtaining production zones from 250 to 600 km, although the bulk of the studies have found zones above 350 km. Rannou et al. (2002) argue for a dynamical origin to the detached haze layer, with a production zone at the level of the detached haze layer around 400 km. Although the dynamical mechanism postulated for the existence of the detached haze layer and polar hood seems plausible, the production zone is placed much higher than where chemistry takes place (Fig. 12). It is unlikely that vertical winds might transport haze precursors from a production zone of 220–400 km before conversion to haze particles, as the chemical timescales are much smaller. The distribution of haze particles in the vertical plane is evidently controlled by eddy diffusion in regions where eddy diffusion is large (Rannou and McKay, 2003). In such a scenario, the high intensity of atmospheric eddies, predicted by this model (Fig. 3a), would act to distribute haze particles both above and below the production zone, which may explain the distribution of the main haze layer. Of course, the particle distribution would also be influenced by coagulation, coalescence, and settling processes. Along with the dynamical explanation for the detached haze layer, nitrile polymerization in the upper atmosphere may also contribute to the detached layer, although it is unclear whether this contribution would be large enough to account solely for the detached layer.

7. Conclusions

The chemical pathways to haze formation in Titan's atmosphere have been analyzed. These pathways include mechanisms involving polyyne, aromatic, and nitrile chemistry, as well as possible mechanisms involving copolymerization, which have been supported by theoretical and laboratory studies. Analysis has involved the inclusion of possible haze pathways in a photochemical model, yielding profiles of haze production sensitive to Titan's atmospheric temperature and pressure.

This analysis has found that the production of haze in Titan's atmosphere is focused in a region around 140–300 km, peaking at an altitude of 220 km. The growth of aromatic molecules is expected to play an important role in the polymerization process, although the nitrile pathway in the form of HCN polymerization, possibly responsible for the orange-brown color of the hazes (Matthews, 1995), may also be significant. It is evident that the spectra of pure poly-HCN do not characterize Titan spectra (Khare et al., 1994), but the combination of PAH and nitrile polymers, as well as possible copolymerization between these two types, may yield different results.

Copolymerization involving HC_3N through aliphatic and aromatic channels are not shown to be significant in haze formation, although the potential provided through the metastable state argues for more kinetic study of this molecule. Furthermore, more attention on the large hydrocarbon radicals like C_4H_3 and n-C_6H_5 and their reactions with stable chemical species would elucidate their role in the polymerization process.

This study highlights the need for more study of reaction kinetics among the PAH, nitrile, and copolymer pathways, in order to identify both rates of reactions and products that might be found by the Cassini-Huygens Gas Chromatograph Mass Spectrometer (GCMS) and Aerosol Collector Pyrolyzer (ACP). Identification of species like naphthalene and nitrile polymer precursors, like n-cyanomethanimine will yield insight into the processes responsible for polymerization.

Acknowledgements

EHW acknowledges support received from the National Research Council Research Associateship Program. SKA acknowledges support received from NASA's Planetary Atmospheres Program, and the Cassini-Huygens GCMS and ACP projects.

References

Allamandola, L.J., Tielens, A.G.G.M., Barker, J.R., 1989. Interstellar polycyclic aromatic hydrocarbons: the infrared emission bands, the excitation/emission mechanism, and the astrophysical implications. Astrophys. J. Suppl. 71, 733–775.

Allen, M., Pinto, J.P., Yung, Y.L., 1980. Titan: aerosol photochemistry and variations related to the sunspot cycle. Astrophys. J. 242, L125–L128.

Banaszkiewicz, M., Lara, L.M., Rodrigo, R., López-Moreno, J.J., Molina-Cuberos, G.J., 2000. A coupled model of Titan's atmosphere and ionosphere. Icarus 147, 386–404.

Bandy, R.E., Lakshminarayan, C., Frost, R.K., Zwier, T.S., 1993. The ultraviolet photochemistry of diacetylene: direct detection of primary products of the metastable $C_4H_2^* + C_4H_2$ reaction. J. Chem. Phys. 98, 5362–5374.

Bar-Nun, A., Kleinfeld, I., Ganor, E., 1988. Shape and optical properties of aerosols formed by photolysis of acetylene, ethylene and hydrogen cyanide. J. Geophys. Res. 93, 8383–8387.

Bauschlicher Jr., C.W., Ricca, A., 2000. Mechanisms for polycyclic aromatic hydrocarbon (PAH) growth. Chem. Phys. Lett. 326, 283–287.

Bézard, B., Drossart, P., Encrenaz, Th., Feuchtgruber, H., 2001. Benzene on the giant planets. Icarus 154, 492–500.

Bittner, J.D., Howard, J.B., 1981. Composition profiles and reaction mechanisms in a near-sooting premixed benzene/oxygen/argon flame. Symp. (Inter.) Combust. 18, 1105–1116.

Burcat, A., Dvinyaninov, M., 1997. Detailed kinetics of cyclopentadiene decomposition studied in a shock tube. Int. J. Chem. Kinet 29, 505–514.

Buss, R.H., Tielens, A.G.G.M., Cohen, M., Werner, M., Bregman, J.D., Witteborn, F.C., 1993. Infrared spectra of transition objects and the composition and evolution of carbon dust. Astrophys. J. 415, 250–257.

Butterfield, M.T., Yu, T., Lin, M.C., 1993. Kinetics of CN reactions with allene, butadiene, propylene, and acrylonitrile. Chem. Phys. 169, 129–134.

Cabane, M., Rannou, P., Chassefière, E., Israel, G., 1993. Fractal aggregates in Titan's atmosphere. Planet. Space Sci. 41, 257–267.

Chassefière, E., Cabane, M., 1995. Two formation regions for Titan's hazes: indirect clues and possible synthesis mechanisms. Planet. Space Sci. 43, 91–103.

Chastaing, D., James, P.L., Sims, I.R., Smith, I.W.M., 1998. Neutral–neutral reactions at the temperatures of interstellar clouds. Rate coefficients for reactions of C_2H radicals with O_2, C_2H_2, C_2H_4 and C_3H_6 down to 15 K. Faraday Discuss. 109, 165–181.

Clarke, D.W., Ferris, J.P., 1995. Photodissociation of cyanoacetylene: application to the atmospheric chemistry on Titan. Icarus 115, 119–125.

Clarke, D.W., Ferris, J.P., 1996. Titan haze: mechanism of cyanoacetylene photochemistry at 185 and 254 nm. J. Geophys. Res. 101, 7575–7584.

Clarke, D.W., Ferris, J.P., 1997. Titan haze: structure and properties of cyanoacetylene and cyanoacetylene–acetylene photopolymers. Icarus 127, 158–172.

Clemett, S.J., Maechling, C.R., Zare, R.N., Messenger, S., Alexander, C.M.O., Gao, X., Swan, P.D., Walker, R.M., 1994. Measurements of aromatic-hydrocarbons in interstellar graphite grains. 2. Molecular measurements. Meteoritics 29, 458.

Coll, P., Coscia, D., Smith, N., Gazeau, M.-C., Ramírez, S.I., Cernogora, G., Israël, G., Raulin, F., 1999. Experimental laboratory simulation of Titan's atmosphere: aerosols and gas phase. Planet. Space Sci. 47, 1331–1340.

Coustenis, A., Bézard, B., Gautier, D., Marten, A., 1989. Titan's atmosphere from Voyager infrared observations. I. The gas composition of Titan's equatorial region. Icarus 80, 54–76.

Coustenis, A., Bézard, B., Gautier, D., Marten, A., Samuelson, R., 1991. Titan's atmosphere from Voyager infrared observations. III. Vertical distributions of hydrocarbons and nitriles near Titan's north pole. Icarus 89, 152–167.

Coustenis, A., Salama, A., Schulz, B., Ott, S., Lellouch, E., Encrenaz, Th., Gautier, D., Feuchtgruber, H., 2003. Titan's atmosphere from ISO mid-infrared spectroscopy. Icarus 161, 383–403.

Derecskei-Kovacs, A., North, S.W., 1999. The unimolecular dissociation of vinylcyanide: a theoretical investigation of a complex multichannel reaction. J. Chem. Phys. 110, 2862–2871.

Ferris, J.P., Guillemin, J.C., 1990. Photochemical cycloaddition reactions of cyanoacetylene and dicyanoacetylene. J. Org. Chem. 55, 5601–5606.

Fink, U., Larson, H.P., 1979. The infrared spectra of Uranus, Neptune, and Titan from 0.8 to 2.5 microns. Astrophys. J. 233, 1021–1040.

Frank, P., Just, Th., 1980. High temperature thermal decomposition of acetylene and diacetylene at low relative concentrations. Combust. Flame 38, 231–248.

Frost, R.K., Zavarin, G.S., Zwier, T.S., 1995. Ultraviolet photochemistry of diacetylene: metastable $C_4H_2^* + C_2H_2$ reaction in helium and nitrogen. J. Phys. Chem. 95, 9408–9415.

Frost, R.K., Arrington, C.A., Ramos, C., Zwier, T.S., 1996. Ultraviolet photochemistry of diacetylene: the metastable $C_4H_2^*$ reaction with ethane, propene, and propyne. J. Am. Chem. Soc. 118, 4451–4461.

Glicker, S., Okabe, H., 1987. Photochemistry of diacetylene. J. Phys. Chem. 91, 437–440.

Halpern, J.B., Miller, G.E., Okabe, H., Nottingham, W., 1988. The UV photochemistry of cyanoacetylene. J. Photochem. Photobiol. A 42, 63–72.

Halpern, J.B., Miller, G.E., Okabe, H., 1989. The reaction of CN radicals with cyanoacetylene. Chem. Phys. Lett. 155, 347–350.

Hidayat, T., 1997. Ph.D. Thesis, University of Paris.

Kerr, J.A., Parsonage, M.J., 1972. Evaluated kinetic data on gas phase addition reactions. Reactions of atoms and radicals with alkenes, alkynes, and aromatic compounds. Butterworths, London.

Khare, B.N., Sagan, C., Thompson, W.R., Arakawa, E.T., Meese, C., Tuminello, P.S., 1994. Optical properties of poly-HCN and their astronomical applications. Can. J. Chem. 72, 678–694.

Kiefer, J.H., von Drasek, W.A., 1990. The mechanism of the homogeneous pyrolysis of acetylene. Int. J. Chem. Kin. 22, 747–786.

Krestinin, A.V., 2000. Detailed modeling of soot formation in hydrocarbon pyrolysis. Combust. Flame 121, 513–524.

Lara, L.M., Lellouch, E., López-Moreno, J.J., Rodrigo, R., 1996. Vertical distribution of Titan's atmospheric neutral constituents. J. Geophys. Res. 101, 23261–23283.

Lara, L.M., Lellouch, E., Shematovich, V., 1999. Titan's atmospheric haze: the case for HCN incorporation. Astron. Astrophys. 341, 312–317.

Lara, L.M., Banaszkiewicz, M., Rodrigo, R., López-Moreno, J.J., 2002. The CH_4 density in the upper atmosphere of Titan. Icarus 158, 191–198.

Lebonnois, S., Toublanc, D., Hourdin, F., Rannou, P., 2001. Seasonal variations of Titan's atmospheric composition. Icarus 152, 384–406.

Lebonnois, S., Bakes, E.L.O., McKay, C.P., 2002. Transition from gaseous compounds to aerosols in Titan's atmosphere. Icarus 159, 505–517.

Marten, A., Hidayat, T., Biraud, Y., Moreno, R., 2002. New millimeter heterodyne observations of Titan: vertical distributions of nitriles HCN, HC_3N, CH_3CN, and the isotopic ratio $^{15}N/^{14}N$ in its atmosphere. Icarus 158, 532–544.

Matthews, C.N., 1995. Hydrogen cyanide polymers: from laboratory to space. Planet. Space Sci. 43, 1365–1370.

McGrath, M., Courtin, R., Smith, T.E., Feldman, P.D., Strobel, D.F., 1998. The ultraviolet albedo of Titan. Icarus 131, 382–392.

McKay, C., Pollack, J.B., Courtin, R., 1989. The thermal structure of Titan's atmosphere. Icarus 80, 23–53.

McKay, C.P., Coustenis, A., Samuelson, R.E., Lemmon, M.T., Lorenz, R.D., Cabane, M., Rannou, P., Drossart, P., 2001. Physical properties of the organic aerosols and clouds on Titan. Planet. Space Sci. 49, 79–99.

Monks, P.S., Romani, P.N., Nesbitt, F.L., Scanlon, M., Stief, L.J., 1993. The kinetics of the formation of nitrile compounds in the atmospheres of Titan and Neptune. J. Geophys. Res. 98, 17,115–17,122.

Monks, P.S., Nesbitt, F.L., Payne, W.A., Scanlon, M., Stief, L.J., Shallcross, D.E., 1995. Absolute rate constants and product branching ratios for the reaction between H and C_2H_3 at $T = 213$ and 298 K. J. Phys. Chem. 99, 17,151–17,159.

Neff, J.S., Ellis, T.A., Apt, J., Bergstralh, J.T., 1985. Bolometric albedos of Titan, Uranus, and Neptune. Icarus 62, 425–432.

Nesbitt, F.L., Marston, G., Stief, L.J., 1990. Kinetic studies of the reactions of H_2CN and D_2CN radicals with N and H. J. Phys. Chem. 94, 4946–4951.

Opansky, B.J., Leone, S.R., 1996a. Low-temperature rate coefficients of C_2H with CH_4 and CD_4 from 154 to 359 K. J. Phys. Chem. 100, 4888–4892.

Opansky, B.J., Leone, S.R., 1996b. Rate coefficients of C_2H with C_2H_4, C_2H_6, and H_2 from 150 to 359 K. J. Phys. Chem. 100, 19904–19910.

Pantos, E., Philis, J., Bolovinos, A., 1978. The extinction coefficient of benzene vapor in the region 4.6 to 36 eV. J. Mol. Spectrosc. 72, 36–43.

Park, J., Burova, S., Rodgers, A.S., Lin, M.C., 1999. Experimental and theoretical studies of the $C_6H_5 + C_6H_6$ reaction. J. Phys. Chem. 103, 9036–9041.

Payne, W.A., Monks, P.S., Nesbitt, F.L., Stief, L.J., 1996. The reaction between $N(^4S)$ and C_2H_3: rate constant and primary reaction channels. J. Chem. Phys. 104, 9808–9815.

Rages, K., Pollack, J.B., 1983. Vertical distribution of scattering hazes in Titan's upper atmosphere. Icarus 55, 50–62.

Rages, K., Pollack, J.B., Smith, P.H., 1983. Size estimates of Titan's aerosols based on Voyager high-phase-angle images. J. Geophys. Res. 88, 8721–8728.

Rannou, P., Cabane, M., Chassefière, E., Botet, R., McKay, C.P., 1995. Titan's geometric albedo: role of the fractal structure of the aerosols. Icarus 111, 355–372.

Rannou, P., Cabane, M., Botet, R., Chassefière, E., 1997. A new interpretation of scattered light measurements at Titan's limb. J. Geophys. Res. 102, 10,997–11,013.

Rannou, P., Hourdin, F., McKay, C.P., 2002. A wind origin for Titan's haze structure. Nature 418, 853–856.

Rannou, P., McKay, C.P., 2003. Fractal models of Titan's haze vertical structure. Planet. Space Sci., doi:10.1016/j.pss.2003.05.08.

Rettig, T.W., Tegler, S.C., Pasto, D.J., Mumma, M.J., 1992. Comet outbursts and polymers of HCN. Astrophys. J. 398, 293–298.

Ricca, A., Bauschlicher Jr., C.W., Bakes, E.L.O., 2001. A computational study of the mechanisms for the incorporation of a nitrogen atom into polycyclic aromatic hydrocarbons in the Titan haze. Icarus 154, 516–521.

Richter, H., Howard, J.B., 2000. Formation of polycyclic aromatic hydrocarbons and their growth to soot—a review of chemical reaction pathways. Prog. Energy Combust. Sci. 26, 565–608.

Sagan, C., Khare, B.N., 1979. Tholins—organic-chemistry of inter-stellar grains and gas. Nature 277, 102–107.

Sagan, C., Khare, B.N., Thompson, W.R., McDonald, G.D., Wing, M.R., Bada, J.L., Vo-Dinh, T., Arakawa, E.T., 1993. Polycyclic aromatic hydrocarbons in the atmospheres of Titan and Jupiter. Astrophys. J. 414, 399–405.

Scattergood, T.W., 1995. The physical nature of Titan's aerosols: laboratory simulations. Adv. Space Res. 15, 313–316.

Scattergood, T.W., Lau, E.Y., Stone, B.M., 1992. Titan's aerosols. Icarus 99, 98–105.

Seki, K., Okabe, H., 1993. Photochemistry of acetylene at 193.3 nm. J. Phys. Chem. 97, 5284–5290.

Seki, K., Nakashima, N., Nishi, N., Kinoshita, M., 1986. Photochemistry of acetylene at 193 nm: Two pathways for diacetylene formation. J. Chem. Phys. 85, 274–279.

Seki, K., Yagi, M., He, M., Halpern, J.B., Okabe, H., 1996. Reaction rates of the CN radical with diacetylene and dicyanoacetylene. Chem. Phys. Lett. 258, 657–662.

Sims, I.R., Queffelec, J.-L., Travers, D., Rowe, B.R., Herbert, L.B., Karthäuser, J., Smith, I.W.M., 1993. Rate constants for the reactions of CN with hydrocarbons at low and ultra-low temperatures. Chem. Phys. Lett. 211, 461–468.

Smith, B.A., et al., 1981. Encounter with Saturn: Voyager 1 imaging science results. Science 215, 504–537.

Suto, M., Lee, L.C., 1985. Photoabsorption cross section of CH_3CN: photodissociation rates by solar flux and interstellar radiation. J. Geophys. Res. 90, 13,037–13,040.

Tanguy, L., Bézard, B., Marten, A., Gautier, D., Gérard, E., Paubert, G., Lecacheux, A., 1990. Stratospheric profile of HCN on Titan from millimeter observations, Icarus, 85, 43–57.

Thompson, W.R., Sagan, C., 1989. Atmospheric formation of organic heteropolymers from $N_2 + CH_4$: structural suggestions for amino acid and oligomer precursors. Origins of Life 19, 503–504.

Toon, O.B., McKay, C.P., Griffith, C.A., Turco, R.P., 1992. A physical model of Titan's aerosols. Icarus 95, 24–53.

Toublanc, D., Parisot, J.P., Brillet, J., Gautier, D., Raulin, F., McKay, C.P., 1995. Photochemical modeling of Titan's atmosphere. Icarus 113, 2–26.

Tran, B.N., Ferris, J.P., Chera, J.J., 2003. The photochemical formation of a Titan haze analog. Structural analysis by X-ray photoelectron and infrared spectroscopy. Icarus 162, 114–124.

deVanssay, E., Gazeau, M.C., Guillemin, J.C., Raulin, F., 1995. Experimental simulation of Titan's organic chemistry at low temperature. Planet. Space Sci. 43, 25–31.

Wang, H., Frenklach, M., 1994. Calculations of rate coefficients for the chemically activated reactions of acetylene with vinylic and aromatic radicals. J. Phys. Chem. 98, 11,465–11,489.

Wang, H., Frenklach, M., 1997. A detailed kinetic modeling study of aromatics formation in laminar premixed acetylene and ethylene flames. Combust. Flame 110, 173–221.

Weissmann, M.A., Benson, S.W., 1988. Rate parameters for the reaction of C_2H_3 and C_4H_5 with H_2 and C_2H_2. J. Phys. Chem. 92, 4080–4084.

Westmoreland, P.R., Dean, A.M., Howard, J.B., Longwell, J.P., 1989. Forming benzene in flames by chemically activated isomerization. J. Phys. Chem. 93, 8171–8180.

Wilson, E.H., 2002. Ph.D Thesis, University of Michigan.

Wilson, E.H., Atreya, S.K., 2001. Mechanisms for the formation of haze in the atmosphere of Titan. Bull. Amer. Astron. Soc. 33, 1139.

Wilson, E.H., Atreya, S.K., 2002. The case for an intermediate homopause level in the atmosphere of Titan. Geophys. Res. Abstr., GRA4.

Wilson, E.H., Atreya, S.K., Coustenis, A., 2003. Mechanisms for the formation of benzene in the atmosphere of Titan. J. Geophys. Res. 108, 5014.

Winnewisser, G., Walmsley, C.M., 1978. Detection of HC_5N and HC_7N in IRC+10216. Astron. Astrophys. 70, L37–L39.

Yang, D.L., Yu, T., Lin, M.C., Melius, C.F., 1992. CN radical reactions with hydrogen cyanide and cyanogen: comparison of theory and experiment. J. Chem. Phys. 97, 222–226.

Yelle, R.V., Strobel, D.F., Lellouch, E., Gautier, D., 1997. Engineering models for Titan's atmosphere. European Space Agency Special Publications ESA SP-1177, pp. 243–256.

Yu, T., Lin, M.C., Melius, C.F., 1994. Absolute rate constant for the reaction of phenyl radical with acetylene. Int. J. Chem. Kin. 26, 1095–1104.

Yung, Y.L., 1987. An update of nitrile photochemistry. Icarus 72, 468–472.

Yung, Y.L., Allen, M., Pinto, J.P., 1984. Photochemistry of the atmosphere of Titan: comparison between model and observations. Astrophys. J. Suppl. 55, 465–506.

Zwier, T.S., Allen, M., 1996. Metastable diacetylene reactions as routes to large hydrocarbons in Titan's atmosphere. Icarus 123, 578–583.